Available online at www.sciencedirect.com
ScienceDirect
Energy 32 (2007) 1724–1730
ENERGY
www.elsevier.com/locate/energy

A detailed modeling method for photovoltaic cells

R. Chenni*, M. Makhlouf, T. Kerbache, A. Bouzid

Department of Electrical Engineering, Faculty of Engineering Sciences, Mentouri University Route d'Ain El Bey, Constantine, Algeria

Received 10 December 2005

Abstract

The photovoltaic cells current–voltage mathematical description is usually defined by a coupled nonlinear equation, difficult to solve using analytical methods. This paper investigates a modeling process configuring a computer simulation model, able to demonstrate the cell's output features in terms of irradiance and temperature environment changes. The model is based on four parameters, and it is tested to simulate three popular types of photovoltaic panels constructed with different materials: copper indium diselenide (CIS) thin film, multi-crystalline silicon, and mono-crystalline silicon. A comparative study of simulation results, carried out by the product manufacturer data, is provided to prove the efficiency of the proposed approach.

Keywords: Solar energy; Photovoltaic panels; Four parameters model; Reverse saturation current; Manufacturer's data

1. Introduction

The performance of solar cell is normally evaluated under the standard test condition (STC), where an average solar spectrum at AM 1.5 is used, the irradiance is normalized to 1000 W/m^2, and the cell temperature is defined as 25 °C. To satisfy the requirement of temperature and insolation in STC, the test usually needs specified environment and some special testing equipment, such as an expensive solar simulator. Simple experiments may not be sufficient to reproduce accurately the solar cell electrical characteristics. In this study, the modeling method is based on the specification data provided in the manufacturers' datasheets.

The primary solar cell equivalent circuit contains a current source with parallel diode, as presented in Fig. 1. A newer topology is adopted in this study. This latter, called the single-diode model or the so-called four-parameter model, includes a photocurrent source, a parallel diode and a series resistor R_S (Fig. 1).

Generally, in case of the single-diode model the four-parameter determination is difficult due to the exponential equation of the diode p–n junction. In Ref. [1], the solar model was developed through the coupled multi-physical photovoltaic energy conversion processes. In [2], the Levenberg–Marquardt method was chosen to solve the double-exponential model equation. To avoid the modeling sophistication, a data-based approach is presented in this paper.

2. Modeling

Applying Kirchoff laws, the cell terminal current is expressed by

$$I = I_L - I_D. \tag{2.1}$$

The light current depends on both irradiance and temperature. It is measured at some reference conditions as written in (2.2) as

$$I_L = \left(\frac{G}{G_{REF}}\right)\left(I_{L,REF} + \mu_{ISC}\left(T_C - T_{C,REF}\right)\right), \tag{2.2}$$

where $I_{L,REF}$ is the light current at reference condition (A); G, G_{REF} the irradiance, actual and at reference condition (W/m^2); T, $T_{C,REF}$ the cell temperature, actual and at reference condition (K); μ_{ISC} the manufacturer supplied temperature coefficient of short-circuit current (A/K).

*Corresponding author. Tel.: +213 31 65 17 47; fax: +213 31 90 13 80.
E-mail address: rachid.chenni@caramail.com (R. Chenni).

0360-5442/$ - see front matter © 2007 Elsevier Ltd. All rights reserved.
doi:10.1016/j.energy.2006.12.006

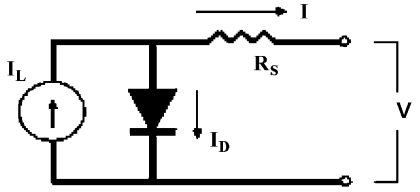

Fig. 1. Equivalent circuit of the four-parameter model.

The diode current is given by Shockley equation

$$I_D = I_0\left[\exp\left(\frac{q(V+IR_s)}{\gamma kT_c}\right)-1\right], \tag{2.3}$$

where V, terminal voltage (V); I, reverse saturation current (A); γ, shape factor; R_s, series resistance (Ω); q, electron charge 1.602×10^{-19} C; k, Boltzmann constant, 1.381×10^{-23} J/K.

The reverse saturation current is

$$I_0 = DT_c^3\exp\left(\frac{-q\varepsilon_G}{AkT_c}\right), \tag{2.4}$$

where D, diode diffusion factor; ε_G, material bandgap energy (1.12 eV for Si, 1.35 eV for GaGs); A , completion factor and $\gamma = A\cdot NCS\cdot NS$.

The reverse saturation current is actually computed by taking the ratio of Eq. (2.4) at two different temperatures, thereby eliminating D. Similar to the determination of I_L, I_0 is related to the temperature and the saturation current estimated at some reference condition

$$I_0 = I_{0,REF}\left(\frac{T_C}{T_{C,REF}}\right)^3\exp\left[\left(\frac{q\varepsilon_G}{kA}\right)\left(\frac{1}{T_{C,REF}}-\frac{1}{T_C}\right)\right]. \tag{2.5}$$

And thus the I–V characteristic is described by

$$I = I_L - I_0\left[\exp\left(\frac{q(V+IR_s)}{\gamma kT_c}\right)-1\right]. \tag{2.6}$$

The shape factor γ is a measure of cell imperfection and is related to the completion factor by

$$\gamma = A\,NCS\,NS, \tag{2.7}$$

where NCS is the number of cells connected in series per module. A module is defined as an array of cells, usually encapsulated for protection, as manufacturer supplies it; NS is the number of modules connected in series of the entire array.

While Rs and γ are assumed to be constant, I_L is a function of irradiance and cell temperature and I_0 is a function of temperature only. The cell temperature can be determined from the ambient temperature and with the help of some standard test information.

For a given irradiance, cell temperature and cell parameters, a continuous relationship of current as a function of voltage is given by Eq. (2.6). It is a nonlinear implicit equation and has to be solved numerically. The typical current–voltage and power–voltage output described by this equation is shown in Fig. 2.

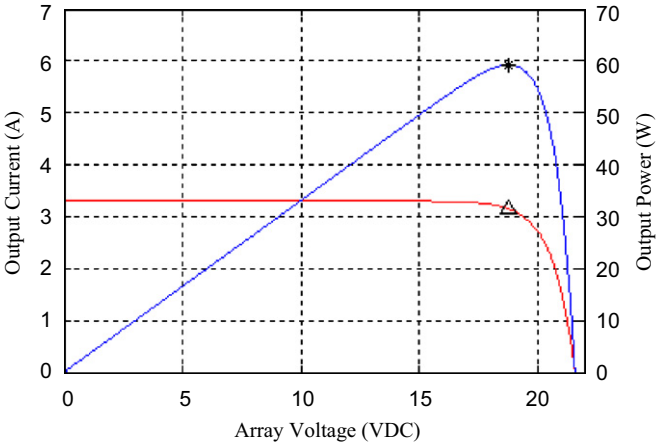

Fig. 2. Current–voltage and power–voltage characteristics.

Looking at the I–V curve, the photovoltaic cell is a constant current source at low voltages with a current approximately equal to the short-circuit current I_{SC}. With increasing voltage at a certain point, the current begins to drop off exponentially to zero at open-circuit voltage V_{OC}. Over the entire voltage range, there is one point where the cell operates at the highest efficiency; this is the maximum power point. The goal of the system design is to operate the cell at that point. However, the system design is complicated by the fact that the maximum power point varies with irradiance and temperature.

A basic factor, which describes the quality of the I–V curve, is the fill factor (FF).

$$FF = \frac{V_{mp}I_{mp}}{V_{oc}I_{sc}}. \tag{2.8}$$

The fill factor is used to compare different solar cells under these same reference conditions.

3. Evaluation of the parameters

Generally, available manufacturer's information are set at three points at the reference conditions: the voltage at open circuit $V_{OC,REF}$, the current at short circuit $I_{SC,REF}$ and the voltage and current at maximum power $V_{MP,REF}$ and $I_{MP,REF}$, the solving method has to force the I–V curve to move around these three points.

The relationships for the given points are: $I = I_{SC}$ and $V = 0$ at short circuit, $I = 0$ and $V = V_{OC}$ at open circuit, $I = I_{MP}$ and $V = V_{MP}$ at maximum power.

Substituting these expressions successively in Eq. (2.7) we obtain the following equation system:

$$I_{sc,ref} = I_{L,ref} - I_{0,ref}\left[\exp\left(\frac{qI_{sc,ref}R_s}{\gamma kT_{c,ref}}\right)-1\right], \tag{3.1}$$

$$0 = I_{L,ref} - I_{0,ref}\left[\exp\left(\frac{qV_{oc,ref}}{\gamma kT_{c,ref}}\right)-1\right], \tag{3.2}$$

$$I_{MP,REF} = I_{L,REF} - I_{0,ref} \times \left[\exp\left(\frac{q\left(V_{MP,REF} + I_{MP,REF}R_S\right)}{\gamma k T_{c,ref}}\right) - 1\right]. \quad (3.3)$$

The reverse saturation current I_0 for any diode is a very small quantity, on the order of 10^{-5} or 10^{-6} A. This minimizes the impact of the exponential term in Eq. (3.1), so it is safe to assume that the photocurrent equals the short-circuit current [3].

Another simplification [4] can be made regarding the first term in Eqs. (3.2) and (3.3). In both cases, regardless of the system size, the exponential term is much greater than the first term. For this reason the first term can be neglected. Then, the equation system becomes

$$I_{L,REF} \approx I_{SC,REF}, \quad (3.4)$$

$$0 \approx I_{SC,REF} - I_{0,REF} \exp\left(\frac{qV_{OC,REF}}{kT_{C,REF}\gamma}\right), \quad (3.5)$$

$$I_{MP,REF} \approx I_{SC,REF} - I_{0,REF} \exp \times \left(\frac{q\left(V_{MP,REF} + I_{MP,REF}R_S\right)}{k\gamma T_{C,REF}}\right). \quad (3.6)$$

Replacing Eq. (3.4) into (3.5) lead to

$$\gamma = \frac{q\left(V_{MP,REF} + I_{MP,REF}R_S - V_{OC,REF}\right)}{kT_{C,REF}\ \ln\left(1 - (I_{MP,REF}/I_{SC,REF})\right)}. \quad (3.7)$$

Finally $I_{0,REF}$ is determined substituting γ into Eq. (3.4),

$$I_{0,REF} = I_{SC,REF} \exp\left(\frac{-qV_{OC,REF}}{k\gamma T_{C,REF}}\right). \quad (3.8)$$

Each of these parameters is evaluated at the reference condition and they are known from the manufacturer's data. For other conditions, I_L may be updated using Eq. (2.2), and I_0 may be recalculated using Eq. (2.5).

4. Series resistor R_s evaluation

The series resistance term proves to be an important parameter, especially for irradiances and cell temperatures far from the reference condition. Given the same set of reference conditions, each *I–V* model traces *I–V* curves that are very similar, but only near the reference conditions. Away from the reference conditions, *I–V* models, including a series resistance term, describe *I–V* curves that are quite different than the curves described by those neglecting this term. Over a full range of operating conditions, such as in an annual simulation, the predicted output (for maximum power tracked systems), when series resistance is neglected ranges from 5% to 8% lower than if the "correct" series resistance is used.

Several different methods have been developed to determine the series resistance. The method used in this study was proposed by Townsend [5]. Among the four methods model, he investigated a method based on an iterative search for a proper value of R_s carrying out best results. The method uses the temperature coefficient of the open-circuit voltage μ_{voc}, often supplied by the manufacturer.

The basic idea behind the procedure is to derive an analytical expression for μ_{voc} using the equation presented in the previous section. As discussed in Section 2, guessing a series resistance fixes the remaining parameters I_0 , γ and I_L (actually I_L is independent on R_s by Eq. (3.4)). The estimated parameters are used to develop an analytical expression for μ_{voc}. The reported and the analytical values of μ_{voc} are compared and a binomial search routine, the bisection method is used to converge on the proper value of μ_{voc} by making new guesses for R_s.

The bisection method requires a lower and an upper limit for the convergence variable, in this case for R_s. The lower limit is chosen to be 0 Ω, the resulting parameters are obtained using Eqs. (3.4), (3.7) and (3.8)

$$I_{L,low} = I_{sc,ref}, \quad (4.1)$$

$$\gamma_{low} = \frac{q\left(V_{mp,ref} - V_{oc,ref}\right)}{kT_{C,REF}\ \ln\left(1 - (I_{mp,ref}/I_{sc,ref})\right)}, \quad (4.2)$$

$$I_{0,low} = I_{sc,ref} \exp\left(\frac{-qV_{oc,ref}}{kT_{C,REF}\gamma_{low}}\right). \quad (4.3)$$

The upper limit for R_s is established by physical limitations. Three points on the *I–V* curve (the open-circuit voltage, the short-circuit current and the maximum power point) are fixed independently of the values of the parameters values, although that these lasts describe curve shape, mainly the shape factor γ. Since R_s fixes the remaining parameters, different values of R_s will affect the curve shape. It is observed that progressively higher values of R_s result in progressively lower values of γ. Thus, the lowest value of γ would determine the upper limit of R_s. The lowest limit of γ is given by the number of series cells *NCS*. Since γ is the product of completion factor A and *NCS*, and A has a low limit of 1.0, the lowest limit of A corresponds to ideal cell behavior, i.e. that each photon-generated electron–hole pair contributes to the cell current rather than recombining. Substituting λ equal to *NCS*, Eq. (3.7) may be rearranged to obtain the upper limit for R_s

$$R_{s,\max} = \frac{1}{I_{mp,ref}}\left[\frac{kT_{C,REF}NCS}{q}\ln\left(1 - \frac{I_{mp,ref}}{I_{sc,ref}}\right) + V_{oc,ref} - V_{mp,ref}\right]. \quad (4.5)$$

The upper limit for I_L is then identical to the lower limit, seen that I_L is not affected by R_s, and I_0 is recalculated according to Eq. (3.8).

The analytical expression for μ_{voc} is obtained by rearranging Eq. (3.5) yielding to

$$V_{oc,ref} = \frac{kT_{C,REF}\gamma}{q}\ln\left(\frac{I_{sc,ref}}{I_{0,ref}}\right). \quad (4.6)$$

And differentiating this expression with respect to cell temperature results in

$$\mu_{voc} = \frac{\partial V_{oc,ref}}{\partial T_{c,ref}} = \frac{\gamma k}{q}\left[\ln\left(\frac{I_{sc,ref}}{I_{0,ref}}\right) + \frac{T_{c,ref}\mu_{isc}}{I_{sc,ref}} - \left(3 + \frac{q\varepsilon_G}{AkT_{c,ref}}\right)\right]. \quad (4.7)$$

This analytical value is compared to the measured value of μ_{voc} and new guesses for R_s are made until the analytical and empirical value are much sufficient. The flow chart software that determines the final value of R_s is shown in Fig. 3.

The effect of the variation in series resistance on I–V behavior is illustrated in Fig. 4.

5. Effect of series/parallel grouping

The power output from single photovoltaic cells is relatively small (approximately 0.5 W). To produce the required voltage and power, photovoltaic cells are connected in series and parallel. They are grouped into modules, the smallest assembly designed to produce DC power and as mentioned before, and the smallest available from manufacturer.

Modules are combined into panels. These panels are connected together to build up the entire photovoltaic array. In this way, any desired I–V characteristic could be generated.

The parameters evaluated in the previous section are based on data input for a single module at some reference condition. To describe the I–V characteristic for the entire array, parameters need be scaled up in the following way:

$$I_{L,tot} = NP\,I_L, \quad (5.1)$$

$$I_{0,tot} = NP\,I_0, \quad (5.2)$$

$$\gamma_{tot} = NS\,\gamma, \quad (5.3)$$

$$R_{Stot} = \frac{NS}{NP}\,R_S, \quad (5.4)$$

where NP and NS are the number of modules connected in parallel and in series, respectively. The effect of series and parallel grouping on the I–V characteristic is shown in Fig. 5. Connecting cells in series will increase the output voltage, and connecting them in parallel will increase the output current, corresponding to the expression

$$I_{tot} = NP\,I, \quad (5.5)$$

$$V_{tot} = NS\,V. \quad (5.6)$$

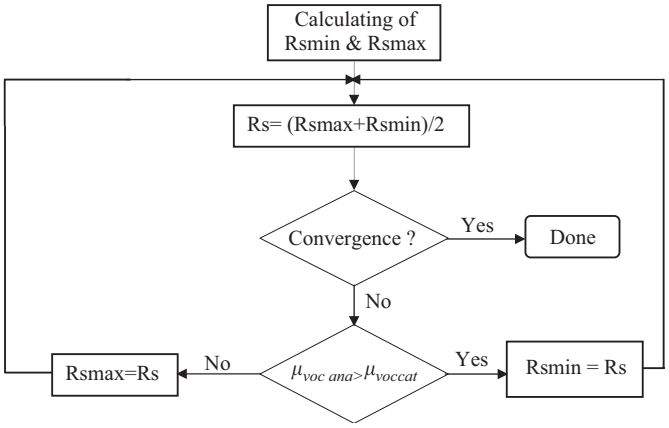

Fig. 3. Software flow chart to determine the final value of R_s.

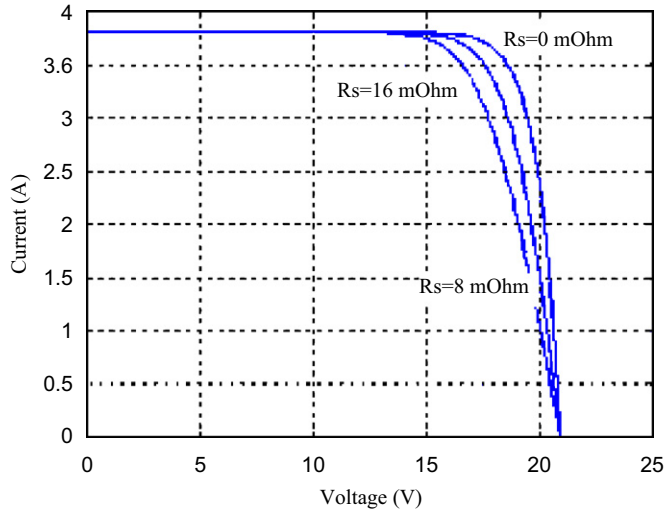

Fig. 4. Effect of variation in series resistance on I–V behavior.

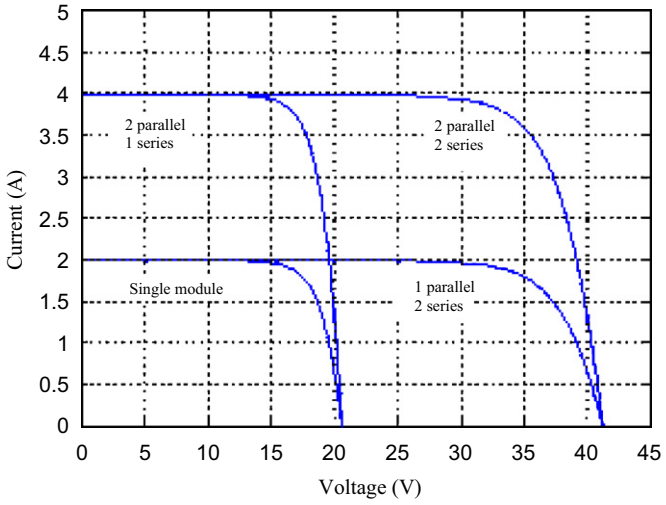

Fig. 5. Effect of series and parallel connection of PV modules on I–V curves.

6. Effect of irradiance and temperature on *I–V* behavior

The response of a photovoltaic cell to different illumination levels is shown in Fig. 6. Obviously, irradiance has a large effect on short-circuit current, i.e. the relatively horizontal arm of the *I–V* curve, while the effect on open-circuit voltage, i.e. the relatively vertical arm of the curve, is rather weak. Regarding the maximum power output of a photovoltaic cell, it is clear that when the irradiance is higher, the cell generates more power.

As mentioned above, the temperature has an effect on the output of a photovoltaic cell. As shown in Fig. 7, increasing the temperature causes the voltage to drop at high voltages. Operating the cell in this region of the curve leads to a significant power reduction at high temperatures. This is a particularly severe problem, since the cell is often operated at the maximum power point, which is within the region. The effect of temperature on short-circuit current is small but increases with irradiance growth.

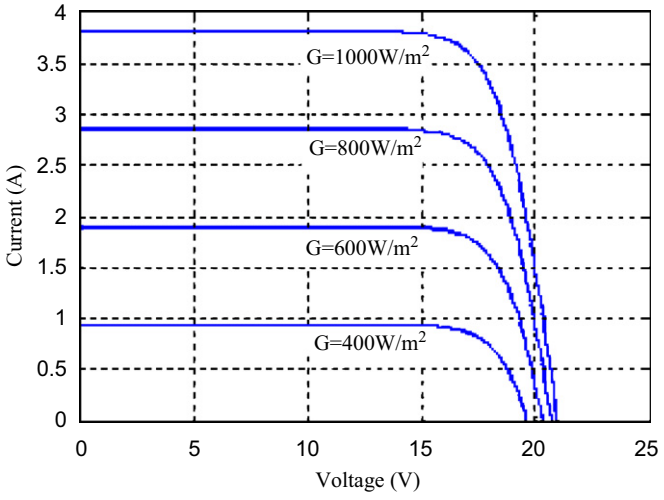

Fig. 6. Effect of irradiance on *I–V* characteristics.

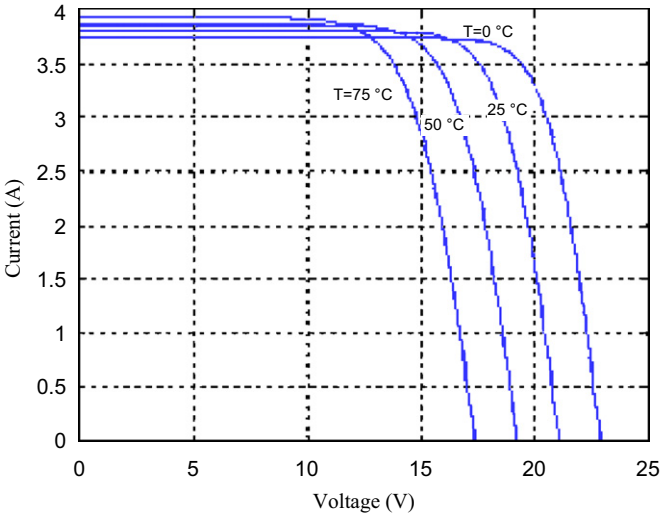

Fig. 7. Effect of temperature on *I–V* characteristics.

7. Determination of cell temperature

In order to predict the energy production of photovoltaic modules, it is necessary to predict the module temperature as a function of ambient temperature, wind speed, total irradiance. As mentioned in Ref. [6] the cell temperature can be determined by the following relationship:

$$T_{module}(^{\circ}\mathrm{C}) = 0.943\,T_{ambiant} + 0.028\,Irradiance - 1.528\,Windspeed + 4.3, \tag{7.1}$$

where $T_{ambient}$ is given in (°C), irradiance in (W/m^2) and wind speed in m/s.

8. Determination of peak-power parameters

At the maximum power point we have

$$\frac{\partial P}{\partial V} = V\,\frac{\partial I}{\partial V} + I = 0. \tag{8.1}$$

With the current described by Eq. (1.6), the partial derivative of I with respect to V is

$$\frac{\partial I}{\partial V} = -I_0\,\exp\left(\frac{q(V+IR_S)}{k\gamma T_{C,REF}}\right)\frac{q}{kT_{C,REF}}\left(1 + R_S\frac{\partial I}{\partial V}\right). \tag{8.2}$$

An explicit expression for $\partial I/\partial V$ is obtained simply by rearranging Eq. (8.2). Back substitution of this explicit expression (8.2) and using I_{MP} for I and V_{MP} for V gives

$$I_L + I_0\,\exp\left(\frac{q(V_{MP}+I_{MP}R_S)}{kT_{C,REF}\gamma}\right) \times\left(1 + \frac{(qV_{MP}/k\gamma T_{C,REF})}{1+\frac{qR_SI_0}{k\gamma T_{C,REF}}\exp\left(\frac{q(V_{MP}+I_{MP}R_S)}{k\gamma T_{C,REF}}\right)}\right) = 0. \tag{8.3}$$

To eliminate V_{MP} in Eq. (8.3), the general *I–V* Eq. (3.6) is used, with I_{MP} substituted for I and V_{MP} substitutes for V. Rearranging to solve for V_{MP} gives

$$V_{MP} = \frac{k\gamma T_{C,REF}}{q}\ln\left(\frac{I_L - I_{MP}}{I_0} + 1\right) - I_{MP}R_S. \tag{8.4}$$

An explicit expression for I_{MP} is obtained by substituting Eq. (8.4) into Eq. (8.3)

$$I_{MP} + \frac{(I_{MP} - I_L - I_0)\left[\ln\left(\frac{I_L - I_{MP}}{I_0}+1\right) - \frac{qI_{MP}R_S}{k\gamma T_{C,REF}}\right]}{1 + (I_L - I_{MP} + I_0)\frac{qR_S}{k\gamma T_{C,REF}}} = 0. \tag{8.5}$$

Newton–Raphson method is applied to solve for I_{MP} using an initial guess given by

$$I_{MP,GUESS} = \frac{G}{G_{REF}}NP\left(I_{MP,REF} + \mu_{ISC}\left(T_C - T_{C,REF}\right)\right). \tag{8.6}$$

Once I_{MP} is found, V_{MP} may be calculated using Eq. (8.4). Thus, the current and voltage at the maximum power point are determined for a given irradiance and cell temperature.

9. Evaluation

There are several types of photovoltaic modules made of various materials. Three types are used to evaluate the effectiveness of the modeling method presented in this paper. Because the open-circuit point (V_{oc}, 0) and short-circuit point (0, I_{sc}) are derived directly from the data given by photovoltaic datasheet, we only need to evaluate the matching accuracy at the different maximum power points.

9.1. CIS thin film

An alternative solar cell technology is thin film, which reduces the material's cost. One of the active materials based on this technology is copper indium diselenide (CIS). The comparison between the simulation and practical data [7] using thin film solar module (Shell ST40) is illustrated in Table 1. The results show that the average relative error on peak-power voltage is 0.67% and the average relative error on peak power is 0.19%.

9.2. Multi-crystalline silicon

The comparison between the simulation and practical data [7] using a typical multi-crystalline solar module (Shell S36) is illustrated in Table 2. The results show that the average relative error on peak-power voltage is 0.22% and the average relative error on peak power is 0.134%.

Table 1
Simulation errors on the maximum power point at different temperature (shell ST40)

Conditions	Data provided by the manufacturers	Simulation results	Relative error (%)
Temperature 50 °C	$P_{MP} = 34.00$ W	$P_{MP} = 34.01$ W	0.02 on P_{MP}
Insolation 1000 W/m^2	$V_{MP} = 14.10$ V	$V_{MP} = 14.13$ V	0.21 on V_{MP}
Temperature 25 °C	$P_{MP} = 40.00$ W	$P_{MP} = 40.05$ W	0.25 on P_{MP}
Insolation 1000 W/m^2	$V_{MP} = 16.60$ V	$V_{MP} = 16.57$ V	0.18 on V_{MP}
Temperature 0 °C	$P_{MP} = 46.00$ W	$P_{MP} = 45.80$ W	0.43 on P_{MP}
Insolation 1000 W/m^2	$V_{MP} = 19.10$ V	$V_{MP} = 19.00$ V	0.52 on V_{MP}
Temperature −25 °C	$P_{MP} = 52.00$ W	$P_{MP} = 51.95$ W	0.09 on P_{MP}
Insolation 1000 W/m^2	$V_{MP} = 21.60$ V	$V_{MP} = 21.20$ V	1.80 on V_{MP}

Table 2
Simulation errors on the maximum power point at different temperature (shell S36)

Conditions	Data provided by the manufacturers	Simulation results	Relative error (%)
Temperature 50 °C	$P_{MP} = 31.95$ W	$P_{MP} = 32.00$ W	0.15 on P_{MP}
Insolation 1000 W/m^2	$V_{MP} = 14.60$ V	$V_{MP} = 14.63$ V	0.20 on V_{MP}
Temperature 25 °C	$P_{MP} = 36.00$ W	$P_{MP} = 36.07$ W	0.19 on P_{MP}
Insolation 1000 W/m^2	$V_{MP} = 16.50$ V	$V_{MP} = 16.55$ V	0.30 on V_{MP}
Temperature 0 °C	$P_{MP} = 40.05$ W	$P_{MP} = 40.09$ W	0.09 on P_{MP}
Insolation 1000 W/m^2	$V_{MP} = 18.40$ V	$V_{MP} = 18.43$ V	0.16 on V_{MP}
Temperature −25 °C	$P_{MP} = 44.10$ W	$P_{MP} = 44.15$ W	0.11 on P_{MP}
Insolation 1000 W/m^2	$V_{MP} = 20.30$ V	$V_{MP} = 20.35$ V	0.24 on V_{MP}

Table 3
Simulation errors on the maximum power point at different temperature (shell SP70)

Conditions	Data provided by the manufacturers	Simulation results	Relative error (%)
Temperature 50 °C	$P_{MP} = 62.13$ W	$P_{MP} = 62.15$ W	0.03 on P_{MP}
Insolation 1000 W/m^2	$V_{MP} = 14.60$ V	$V_{MP} = 14.65$ V	0.34 on V_{MP}
Temperature 25 °C	$P_{MP} = 70.00$ W	$P_{MP} = 69.98$ W	0.02 on P_{MP}
Insolation 1000 W/m^2	$V_{MP} = 16.50$ V	$V_{MP} = 16.53$ V	0.18 on V_{MP}
Temperature 0 °C	$P_{MP} = 77.88$ W	$P_{MP} = 77.90$ W	0.02 on P_{MP}
Insolation 1000 W/m^2	$V_{MP} = 18.40$ V	$V_{MP} = 18.35$ V	0.27 on V_{MP}
Temperature −25 °C	$P_{MP} = 85.75$ W	$P_{MP} = 85.70$ W	0.05 on P_{MP}
Insolation 1000 W/m^2	$V_{MP} = 20.30$ V	$V_{MP} = 20.20$ V	0.49 on V_{MP}

9.3. Mono-crystalline silicon photovoltaic module

The comparison between the simulation and practical data using a typical mono-crystalline solar module (Shell SP70) is illustrated in Table 3. The results show that the average relative error on peak-power voltage is 0.32% and the average relative error on peak power is 0.03%.

10. Conclusion

In this paper, a general approach on modeling photovoltaic modules is presented. The chosen points for the parameters determination under reference conditions are mainly: the short-circuit current (0, $I_{sc,ref}$), the open-circuit voltage point (0, $V_{oc,\mathrm{ref}}$), the temperature coefficient of open-circuit voltage μ_{voc}, the temperature coefficient of short-circuit current μ_{isc} and the maximum power point ($I_{mp,ref}$, $V_{mp,ref}$). The data needed for the model are from either the products' data sheet or experimental testing results. Three types of solar module (CIS thin film, *m*-Si and *c*-Si) were modeled and evaluated. The model accuracy is also analyzed through comparison between product's data and simulation results. The evaluation proves the efficiency of this modeling method based on the four-parameter model.

References

[1] Liu S, Dougal RA. Dynamic multiphysics model for solar array. IEEE Trans Energy Convers 2002;17(2):285–94.
[2] Cow A, Manning CD. Development of a photovoltaic array model for use in power-electronics simulation studies. IEE Proc Electron Power Appl 1999;146(2):193–200.
[3] Bryan F. Simulation of grid-tied building integrated photovoltaic systems. MS thesis, Solar Energy Laboratory, University of Wisconsin, Madison, 1999.
[4] Eckstein, J. H. Detailed modeling of photovoltaic components. MS thesis, Solar Energy Laboratory, University of Wisconsin, Madison, 1990.
[5] Townsend, T. U. A method for estimating the long-term performance of direct-coupled photovoltaic systems. MS Thesis, Solar Energy Laboratory, University of Wisconsin, Madison, 1989.
[6] TamizhMani G, Ji L, Tang Y, Petacci L. Photovoltaic module thermal-wind performance: Long-term monitoring and model development for energy rating. NCPV and solar program review meeting, 2003.
[7] Shell Solar Product Information Sheets.